JOURNAL OF MATERIALS SCIENCE **37** (2002) 343 – 348

Sol-emulsion-gel synthesis of hollow mullite microspheres

M. K. NASKAR, M. CHATTERJEE*
Sol-Gel Division, Central Glass & Ceramic Research Institute, Calcutta 700 032, India
E-mail: minati33@hotmail.com

N. S. LAKSHMI
Department of Physics, Ethiraj College for Women, Chennai, India

Hollow mullite microspheres were obtained from emulsified diphasic sols by an ion extraction method. The surfactant concentration and viscosity of the sols were found to affect the characteristics of the derived microspheres. The gel and calcined microspheres were investigated by using thermogravimetry analysis (TGA), differential thermal analysis (DTA), Fourier transformed infrared spectroscopy (FTIR), X-ray diffraction (XRD), optical and scanning electron microscopy (SEM) and particle size analysis. TGA indicated the removal of most of the volatiles, i.e. 30.77 wt% up to about 500°C. Crystallization of the Si-Al spinel at 900°–970°C in gel microspheres was confirmed by DTA and XRD. XRD results also showed the formation of orthorhombic mullite at 1200°C. FTIR indicated the sequence of transformations taking place during heat-treatment of gel microspheres at different temperatures. The optical and scanning electron microscopy confirmed the spherical morphology of the gel and calcined particles. Formation of hollow microspheres with a single cavity was identified by SEM. The particle size distribution of the mullite microspheres calcined at 1300°C/1h exhibited a size range of 6–100 μm with an average particle size (d_{50}) of 22.5 μm. © *2002 Kluwer Academic Publishers*

1. Introduction

Synthesis of mullite is becoming increasingly important due to applications in structural, electronic and optical fields [1–3] because of some special properties like low thermal expansion [3–5], high creep resistance [3, 5–7], low dielectric constant and good transmissivity in the mid-infrared range [2]. Besides the above applications, hollow mullite microspheres can be used as a feed material for plasma sprayed coatings, thermal insulator, light weight fillers in composites and internal confinement fusion of nuclear materials etc [8, 9]. In sol-gel process the mixing scale i.e. molecular or colloidal level is important in controlling the phase transformation sequence of mullite. On the basis of alumina-silica mixing scale, sol-gel mullite precursors can be categorized into single phase and diphasic gels [10, 11]. There are different techniques of producing hollow ceramic microspheres, namely dual-nozzle hollow drop generation [12], spray pyrolysis [13], emulsion-evaporation technique [14], emulsion-water extraction [8] and emulsion-ion extraction technique [15] etc.

Basically, both the techniques, i.e. emulsion-water extraction and emulsion-ion extraction are known as the sol-emulsion-gel method, as both involves the formation of gel microspheres from the emulsified sol droplets. However, the mechanism of the formation of gel microspheres in the two methods are totally different. In the emulsion-water-extraction technique, the emulsified sol droplets are transformed into the gel microspheres by the extraction or removal of water from the aqueous sol droplets by a suitable dehydrating liquid, e.g. alcohols, while in the emulsion-ion extraction technique (the present method), the stabilizing ion, i.e. the NO_3^- in the present case, in the aqueous sol droplets are extracted with an organic amine, thereby increasing the basicity of the system and resulting in the formation of gel microspheres.

In the present investigation, an attempt has been made (i) to synthesize hollow mullite microspheres by an emulsion-ion extraction technique (instead of water extraction), a more advantageous process in respect of high yield and small processing time [15] and (ii) to examine the conditions of hollow monodisperse sphere formation and their crystallization behaviour. A polymerized alumina sol and a colloidal silica sol (Ludox) have been used as precursors for the synthesis of mullite microspheres.

2. Experimental procedure

2.1. Preparation of an alumina-silica sol

The starting material for the preparation of polymerized alumina sol was $Al(NO_3)_3 \cdot 9H_2O$ (A.R., E. Merck India, purity 99%). An aqueous alumina sol was

---

[*] Author to whom all correspondence should be addressed.

prepared [16] by dissolving the nitrate in deionized water, adjusting the pH value to about 3 by the addition of concentrated ammonia solution (25 wt%, G.R., E. Merck, India) and finally, heating the 1M solution thus obtained to 80°C under controlled condition, i.e. by dropwise addition of concentrated ammonia solution under vigorous stirring in a covered container. During heat-treatment, the viscosity of the resulting sol increased. The pH and the viscosity of the starting alumina sol was 2.91 and 5 ± 1 mPa s respectively. A colloidal silica sol (Ludox, Dupont, De Nemours) containing about 30 wt% SiO_2 (pH∼ 8) was slowly added to the alumina sol under stirring. The molar ratio of alumina to silica in the bi-component (parent) sol was maintained at 3 : 2. The pH and viscosity of the parent sol was 3.96 and 4.5 ± 1 mPa s respectively. From the parent sol, several sols of viscosities ranging from 15 to 60 mPa s were prepared by solvent evaporation. The pH of the sols was measured with a Jencons pH meter (Model 3030) while the viscosity values were recorded using a Brookfield viscometer (Model LVTDV-II).

2.2. Preparation of emulsions

In the present investigation, water-in oil (W/O) type emulsions were prepared [16–19]. The sols prepared as in Section 2.1 above were used as the aqueous phase (W) while an organic solvent, i.e. the cyclohexane (G.R., E. Merck, India) of dielectric constant 2.042 at 25°C [20] was used as the oil phase (O). A mixture of cyclohexane and surfactant (Span 80, Fluka) with a HLB (hydrophilic/lipophilic balance) value of 4.3 acted as the support solvent. The emulsions were prepared by dispersing the sol as droplets in the support solvent under constant agitation (150 rpm). The volume ratio of the sol: support solvent was kept constant at 1:4 in all experiments.

2.3. Preparation of gel and oxide microspheres

The emulsified sol droplets were converted to gel microspheres by the addition of an organic amine (extractant or gelling agent) e.g. triethylamine (TEA) [15–18] under agitation until a pH of 8–9 was reached. The volume ratio of the sol to the gelling agent was about 1 : 0.5. The gel microspheres, after separating by filtration, were washed with acetone (G.R., E. Merck, India) and methanol (G.R., E. Merck, India), dried at 110°C in air under static condition and finally calcined at 1300°C with 1h dwell time (in air under static condition). The characteristics of the sols and the calcined microspheres have been presented in Table I. The gel spheres obtained in the present investigation may be considered as the diphasic gels [10, 11, 21]. The washed gel microspheres corresponding to Run no. 4 of Table I were calcined at different temperatures, i.e. 500°–1300°C (Table II) in air under static condition with different dwell time, i.e. 1–20 h for examining the effect of calcination temperature on powder characteristics.

TABLE I Characteristics of the sols and the oxide particles at 1300°C/1h

Run no.	Span 80 (vol%)	Viscosity (mPa · s)	Optical microscopic results
1	2	15 ± 1	Very little spheres (4–10 μm) + irregular particles
2	2	20 ± 1	Spheres (4–12 μm) + broken spheres
3	2	25 ± 1	Almost all spheres (5–80 μm)
4	2	30 ± 1	Almost all spheres (6–100 μm)
5	2	35 ± 1	Mostly spheres (10–120 μm) + some broken spheres
6	2	45 ± 1	Spheres (20–150 μm) + broken spheres
7	2	60 ± 1	Deformed spheres + broken particles
8	2.5	15 ± 1	Very little spheres (5–10 μm) + irregular particles
9	2.5	20 ± 1	Spheres (5–10 μm) + irregular particles
10	2.5	25 ± 1	Spheres (5–60 μm) + broken spheres
11	2.5	30 ± 1	Spheres (10–90 μm) + broken spheres
12	2.5	35 ± 1	Deformed spheres
13	2.5	45 ± 1	Deformed spheres + irregular particles
14	2.5	60 ± 1	All irregular particles
15	3.0	30 ± 1	Deformed spheres

TABLE II Crystal phases in the oxide microspheres at different temperatures

Sample identification	Calcination temperature (°C)	Dwell time (h)	Crystalline phase by XRD
M0	30	-	Gel microspheres (Amorphous)
M1	500	1	Amorphous
M2	600	1	Amorphous
M3	700	1	Amorphous
M4	800	1	Amorphous
M5	900	1	Si-Al spinel + amorphous silica
M6	1000	1	Si-Al spinel + amorphous silica
M7	1100	1	Si-Al spinel + amorphous silica
M8	1200	1	Si-Al spinel
M9	1250	1	Orthorhombic mullite
M10	1300	1	Orthorhombic mullite
M11	1100	5	Si-Al spinel + amorphous silica
M12	1100	10	Si-Al spinel + amorphous silica
M13	1100	20	Orthorhombic mullite + Si-Al spinel
M14	1200	5	Orthorhombic mullite

2.4. Characterization of the microspheres

The gel and the calcined microspheres were characterized by DTA and TG (404 Netzsch), FTIR study (Nicolet, 5PC), XRD (Philips PW-1730 X-ray unit) with Ni-filtered Cu K_α radiation, optical microscopy (Prior Swift B3000)), SEM (S 430) and particle size analysis (Sedigraph, MM5100, Micromeritics).

3. Results and discussion

3.1. Formation of spherical particles

The sol-emulsion-gel method involves emulsification of an aqueous sol (i.e. "water phase") with high dielectric constant in an organic solvent (i.e. the "oil phase") of low dielectric constant by agitation. The sol droplets are gelled by increasing the basicity of the system

[15–18, 22]. The high interfacial tension between the "water phase" and the "oil phase" is generally reduced according to necessity by the addition of an amphiphilic surface active agent or surfactant, i.e. molecule with a polar head and a non-polar tail [19]. The surfactant molecules orient themselves according to the polarities of the involved chemical constituents. Thus, due to the high polarity of water, the polar heads of the surfactant molecules at the water-oil interface are oriented towards the water droplets. These surfactants are characterized by their HLB values [19].

The HLB values of different non-ionic surfactants in the Span and Tween series have been found to exhibit an inverse relationship to the the average particle size (d_{50}) of microspheres in an earlier investigation [23]. The surfactants in the Tween series are basically the fatty acid esters of anhydro-sorbitols [19] which are made water soluble by etherifying the free hydroxyl groups with ethylene oxide, e.g. polyoxyehylene sorbitan monooleate (Tween 80), polyoxyehylene sorbitan monostearate (Tween 60) etc. When they are not etherified, they become good oil soluble emulsifying agents and constitute the Span series surfactants, e.g. sorbitan monooleate (Span 80), sorbitan monopalmitate (Span 40) etc. In fact, a high HLB value of the surfactant indicates strongly hydrophilic character while a low value is an indication of a strong hydrophobic nature [19, 23]. Considering these points, a non-ionic, relatively pH independent hydrophobic surfactant, i.e. sorbitan monooleate (Span 80) with a HLB value of 4.3 [15–19, 22] was selected for the present study. Fig. 1 shows the molecular structure of the amphiphilic Span 80 [23] where the hydrophilic sorbitan group acts as the "polar head" and the hydrophobic oleic acid group acts as the "non-polar tail".

Table I presents the nature of the oxide particles obtained from the sols of different viscosities. Addition of 2.5 vol% and above of the surfactant was not effective for monodisperse sphere formation. The formation of gel microspheres may be explained to be due to the adsorption of the surfactant molecules at the interface of the aqueous sol droplets and the organic solvent, causing a decrease in the interfacial tension, increasing the stability of the droplets by steric hindrance and thereby preventing their coalescence [19]. A volume ratio of the sol to the gelling agent (extractant) of about 1 : 0.5 in the present method (in contrast to the water extraction technique [8] where the above ratio was 1 : 15) helped to increase the yield of the product in a fixed volume.

3.2. Thermal analysis

The TGA study of the gel microspheres (product of Run no. 4 of Table I) from 30° to 1400°C (10°C/min) showed that the weight losses due to volatilization of water, decomposition of residual nitrates and other organics mostly occurred up to about 500°C accompanying by a weight loss of 30.77% (Fig. 2a). An insignificant amount of weight loss (1.39%) was found from 500° to 1400°C. In the DTA curve (Fig. 2b) of the same sample from 30° to 1400°C (10°C/min), a strong endothermic peak appeared at about 165°C was due to the expulsion of loosely bound water molecules and some organics associated with the material. A small endothermic peak at about 424°C indicated the decomposition of nitrates and structural water molecules [24]. An exothermic peak at about 970°C may be due to the crystallization of Si - Al spinel in diphasic gels [11, 21, 25] suggesting slow reaction of SiO_2 and Al_2O_3. Appearance of another exothermic peak at about 1260°C indicated the crystallization of orthorhombic (o-) mullite [11, 21, 25]. Formation of Si-Al spinel and o-mullite can be supported from the XRD results as discussed in Section 3.3. No other peaks were observed during heating up to 1400°C.

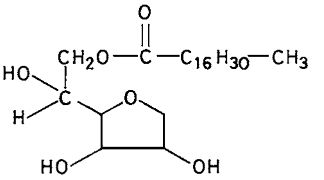

Figure 1 Molecular structure of Span 80 showing the hydrophilic "head" (sorbitan) and the hydrophobic "tail" (oleic acid) parts.

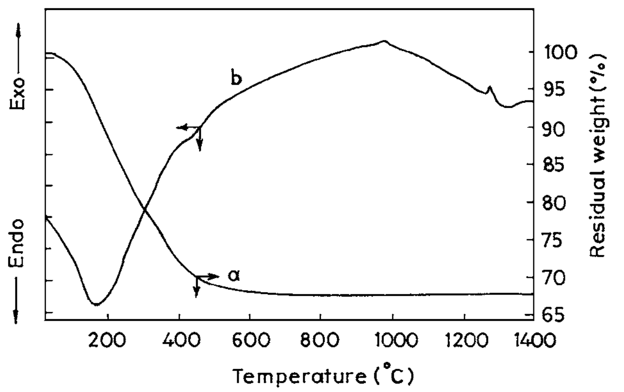

Figure 2 TG (Fig. 2a) and DTA (Fig. 2b) traces of the gel microspheres (Product of Run no. 4 of Table I).

3.3. Crystallization behaviour of the microspheres

Crystalline phases identified by XRD in microspheres calcined at different temperatures have been presented in Table II. The gel microspheres calcined up to 800°C were found to be amorphous in nature [25, 26] which indicates that crystallization of both the alumina and silica polymorphs have been hindered in the present system. However, poor crystallization of Si - Al spinel along with amorphous silica was observed at 900°C/1h. The formation of Si - Al spinel was also indicated in the DTA curve at 970°C (first exothermic peak of Fig. 2b) for the same sample (Section 3.2). Development of Si - Al spinel phase increased with increase in temperature from 900° to 1200°C, each with 1h dwell time. Phase pure orthorhombic (o) mullite was however, obtained with further increase in temperature to 1250°C with 1 h dwell time.

It is to be noted that the orthorhombic mullite was also obtained at somewhat lower temperature, i.e. 1200°C by increasing the dwell time from 1h to 5 h. On the other hand, at 1100°C, even with a maximum dwell time of 20 h, Si - Al spinel was associated with the orthorhombic mullite phase. So, the pathway of crystallization of the precursor gel microspheres in the present study may be represented as follows:

$$\underset{\text{microspheres}}{Al_2O_3 - SiO_2\text{gel}} \rightarrow \text{Si - Al spinel} \rightarrow \underset{\text{(o) mullite}}{\text{Orthorhombic}}$$

3.4. FTIR spectroscopic study

FTIR transmission spectroscopic analysis was performed in both the gel and oxide microspheres of the product of Run no.4 (Table I) and those calcined at different temperatures (Table II) in the wavenumber range 4000–400 cm^{-1} The spectra of different absorption bands are shown in Fig. 3. Absorption band at 1380 cm^{-1} for gel microspheres (M0) was assigned to the presence of residual nitrate groups [15, 27, 28] in the precursor materials. The appearance of absorption bands at around 1120, 550 and 470 cm^{-1} were present in all the samples M0, M5, M6, M7, M8 and M10. These were the characteristic bands of Si - O stretching, Al - O stretching and O - Si - O bending vibration respectively [29]. In addition to those bands, new vibration bands at 825 and 730 cm^{-1} assigned to Al - O bending vibration [27] in alumina tetrahedra (AlO_4) appeared in the sample M8. It indicated that at 1200°C, reaction for mullitization started and Si^{4+} replaced Al^{3+}, positioning in AlO_4 tetrahedra [25]. Further increase in calcination temperature up to 1300°C (M10), mullitization reaction completed with the appearance of new additional absorption bands at 1175 and 897 cm^{-1} indication Al - O stretching vibration in AlO_4 tetrahedra. It is to be noted that in the sample (M10), absorption band at 1175 cm^{-1} was stronger than that of 1120 cm^{-1}; it could be due to the stoichiometric aluminium concentration in mullite composition [30, 31].

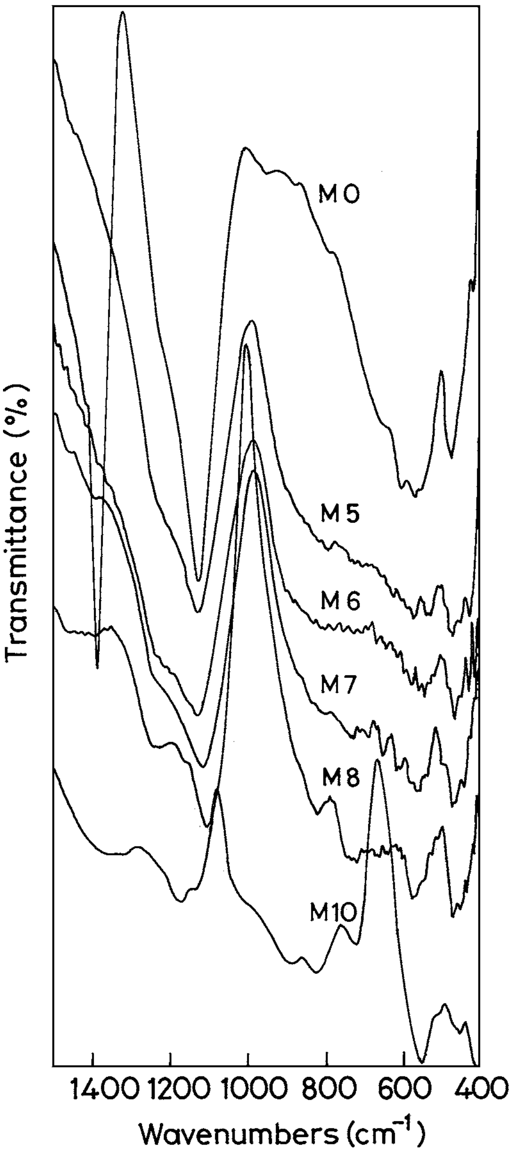

Figure 3 FTIR spectra of gel microspheres (Product of Run no. 4 of Table I) calcined at different temperatures (Table II).

3.5. Optical and scanning electron microscopy

The morphology of the products obtained under different experimental conditions presented in Table I was initially examined with an optical microscope. It is to be noted that sol-gel derived mullite powders (Run nos. 3 and 4) were mostly spherical in morphology (Fig. 4) and the sphericity was retained even after calcination at 1300°C (1h).

The oxide microspheres of Run nos. 3, 4 and 6, all calcined at 1300°C/1h of Table I were examined under SEM. The following observations are made.

(i) The oxide microspheres of Run nos. 3 and 4 obtained from sols of viscosity 25–30 mPa s (Table I) contained very few hollow broken particles (Fig. 5). The broken particles contained a single spherical pore.

(ii) The oxide microspheres of Run no. 6 derived from a sol of high viscosity, i.e. 45 ± 1 mPa s showed that microspheres of size less than about 17 μm did not break, but those larger than about 17 μm were found to be mostly broken (Fig. 6). The fractured microspheres were found hollow with a single spherical cavity. The formation of hollow mullite microspheres in the present study may be explained by the mechanism established for the generation of hollow alumina microspheres in an earlier investigation [15].

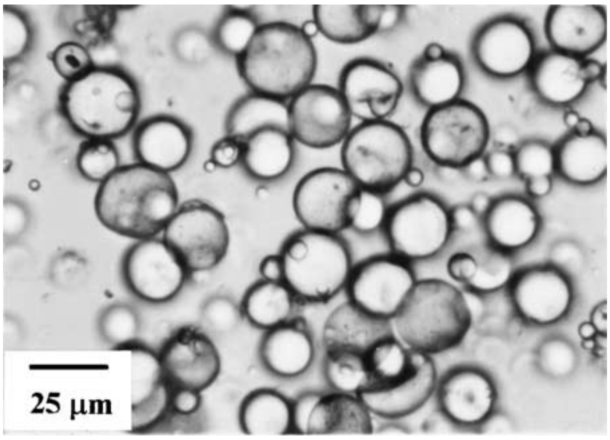

Figure 4 Optical micrograph showing the morphology of crystallized orthorhombic mullite microspheres calcined at 1300°C/1h (Product of Run no. 4 of Table I).

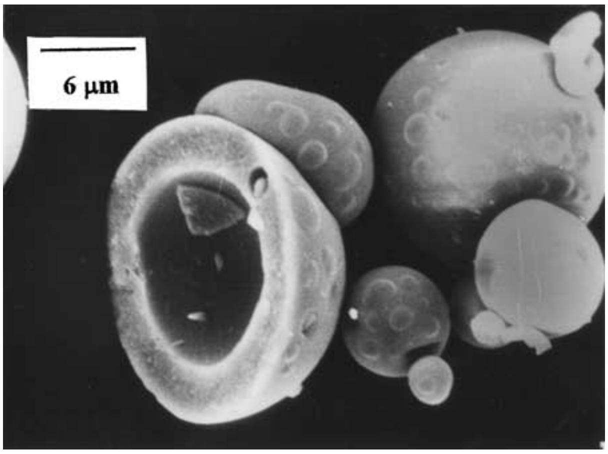

Figure 5 Scanning electron micrograph of a fractured hollow microsphere of orthorhombic mullite with a single cavity obtained at 1300°C/1h (Product of Run no. 4 of Table I).

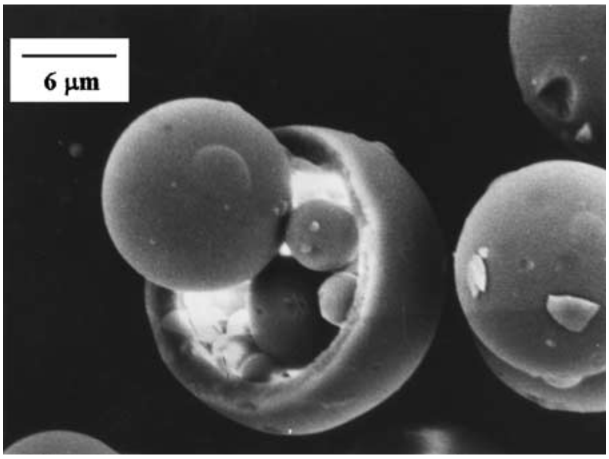

Figure 6 Scanning electron micrograph of orthorhombic mullite (calcined at 1300°C/1h) showing small unbroken microspheres along with a large broken hollow microsphere with a single spherical pore (Product of Run no. 6 of Table I).

In case of the microspheres obtained from the low viscosity and low equivalent oxide content sol, the shell formation with less dense network and high permeability to both TEA and cyclohexane is believed to occur towards the interior part of the droplet, making the shell formation process complete [15]. Repeated washings of these microspheres through a Buchner system under vacuum with methanol and acetone (Section 2.3), help the trapped liquid to come out gradually with the washing solvent through the highly permeable shell [15]. Final removal of the washing solvent under vacuum forms gel microspheres with the internal cavity devoid of any trapped liquid, or containing negligible amount of liquid. During calcination of the washed gel microspheres, the trapped liquid, if any, vaporizes and the vapours are expected to get a passage for their removal through the permeable shell. Under such conditions, formation of unbroken and hollow oxide microspheres (Fig. 5) takes place [15, 32, 33].

In case of microspheres obtained from a sol of high viscosity and high equivalent oxide content, formation of a dense and low permeable shell is believed to occur after complete shell formation [15]. During calcination of these washed microcapsules, the escape of the volatiles formed from the entrapped liquid is expected to be hindered, thus giving rise to a build-up of internal pressure causing fracture of the microspheres [32–34] (Fig. 6). Microspheres of size less than about 17 μm did not break. The particles may be either solid or may contain little porosity [32, 34].

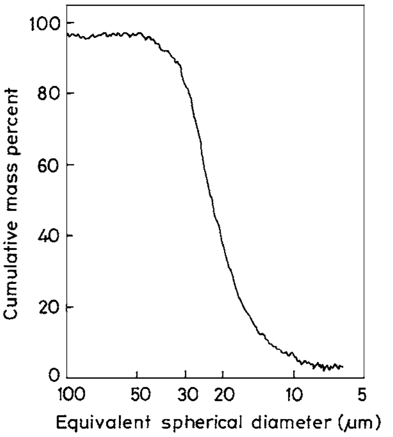

Figure 7 Particle size distribution of orthorhombic mullite microspheres calcined at 1300°C/1h (Product of Run no. 4 of Table I).

3.6. Particle size distribution

The oxide microspheres of Table I observed under the optical microscope indicates that the particle size increased with the increase in viscosity of the sols. Under a given speed of agitation, the sol with a relatively low viscosity along with the low degree of polymerization can be effectively broken into smaller droplets which after gelation and subsequent calcination finally produced particles of smaller size [8]. Fig. 7 shows a typical particle size distribution of the mullite microspheres calcined at 1300°C/1h (product of Run no. 4 of Table I) which shows a size range of 6–100 μm with an average particle size (d_{50}) of 22.5 μm. Thus under a constant speed of agitation, mullite microspheres of the desired particle size distribution can be easily affected by changing the characteristics of the sols.

4. Conclusions

1. The sol-emulsion-gel method can be used for the preparation of hollow mullite microspheres from diphasic sols consisting of polymerized alumina and colloidal silica sols. The gel microspheres are obtained from emulsified sols by an ion extraction method. Calcination of gel microspheres at 1200°C produces hollow mullite microspheres.

2. The gel and calcined microspheres are characterized by DTA, TG, FTIR, XRD, optical and scanning electron microscopy and particle size analysis. Crystallization of the Si-Al spinel at 900°–970°C in the gel microspheres has been confirmed by DTA and XRD. Formation of orthorhombic mullite occurs at 1200°C.

3. The optical and scanning electron microscopy confirm the spherical morphology of the gel and calcined particles. Formation of hollow microspheres with a single cavity has been identified by SEM.

Acknowledgements

The authors thank Dr. H. S. Maiti, Director of the Institute, for his kind permission to publish this paper. They also thank Dr. D. Ganguli, Head, Sol-Gel Division for constant encouragement and providing valuable suggestions regarding this work. Thanks are also due to the members of the Technical Ceramics, Refractories, SEM and finally X-ray Divisions for rendering help in characterization of the powders. One of the authors (N. S. Lakshmi) is thankful to Tamilnadu State Council for Science and Technology for the Young Scientist Fellowship during which some of the work was carried out.

References

1. H. SCHNEIDER, K. OKADA and J. A. PASK, "Mullite and Mullite Ceramics" (John Wiley & Sons, Chichester, 1994).
2. I. A. AKSAY, D. M. DABBS and M. SARIKAYA, *J. Amer. Ceram. Soc.* **74** (1991) 2343.
3. H. SCHNEIDER and E. EBERHARD, *ibid.* **73** (1990) 2073.
4. W. D. KINGERY, H. K. BOWEN and D. R. UHLMAN, "Introduction to Ceramics," 2nd edn. (Wiley, New York, 1975).
5. H. SCHNEIDER, B. SARUHAN, D. VOLL, L. MERWIN and A. SEBALD, *J. Eur. Ceram. Soc.* **11** (1993) 87.
6. P. A. LESSING, R. S. GORDON and K. S. MAZDIYASNI, *J. Amer. Ceram. Soc.* **58** (1979) 149.
7. H. SCHNEIDER, L. MERWIN and A. SEBALD, *J. Mater. Sci.* **27** (1992) 805.
8. J. G. LIU and D. L. WILCOX, SR., *J. Mater. Res.* **10** (1995) 84.
9. R. L. DOWNS, M. A. EBNER and W. J. MILLER, "Sol-Gel Technology for Thin Films, Fibres, Preforms, Electronics and Specialty Shapes," edited by L. C. Klein (Noyes Publications, Park Ridge, USA, 1988) p. 338.
10. S. KOMERNENI, Y. SUWA and R. ROY, *J. Amer. Ceram. Soc.* **69** (1986) c-155.
11. D. W. HOFFMAN, R. ROY and S. KOMERNENI, *ibid.* **67** (1984) 468.
12. K. K. KIM, K. Y. JANG and R. S. UPADHYE, *J. Amer. Ceram. Soc.* **74** (1991) 1987.
13. A. M. GADALLA and H.-F. YU, *J. Mater. Res.* **5** (1990) 2923.
14. Y. SARIKAYA and M. AKINC, *Ceram. Int.* **14** (1988) 239.
15. M. CHATTERJEE, D. ENKHTUVSHIN, B. SILADITYA and D. GANGULI, *J. Mater. Sci.* **33** (1998) 4937.
16. J. RAY, M. CHATTERJEE and D. GANGULI, *J. Mater. Sci. Lett.* **12** (1993) 1755.
17. M. CHATTERJEE, J. RAY, A. CHATTERJEE, D. GANGULI, S. V. JOSHI and M. P. SRIVASTAVA, *J. Mater. Sci.* **28** (1993) 2803.
18. M. CHATTERJEE, B. SILADITYA and D. GANGULI, *Mater. Lett.* **25** (1995) 261.
19. D. GANGULI and M. CHATTERJEE, "Ceramic Powder Preparation:A Handbook" (Kluwer Academic Publishers, Boston, USA, 1997).
20. "Handbook of Chemistry and Physics," edited by D. R. Lide (CRC Press, London, 1994) 75th edn., p. 6.
21. A. K. CHAKRAVORTTY, *J. Thermal Analysis* **46** (1996) 1413.
22. J. L. WOODHEAD, *J. Mater. Edu.* **6** (1984) 887.
23. M. CHATTERJEE, M. K. NASKAR, B. SILADITYA and D. GANGULI, *J. Mater. Res.* **15** (2000) 176.
24. B. TAKAYUKI, H. SHIGEO, A. YASUMORI and K. OKADA, *J. Eur. Ceram. Soc.* **16** (1996) 127.
25. Y. WANG and W. J. THOMSON, *J. Mater. Sci.* **34** (1999) 3577.
26. A. K. CHAKRAVORTY and D. K. GHOSH, *J. Amer. Ceram. Soc.* **70** (1987) c-46.
27. R. L. OREFICE and W. L. VASCONCELOS, *J. Sol-Gel Sci. Technol.* **9** (1997) 239.
28. K. NAKAMOTO, "Infrared and Raman Spectra of Inorganic and Co-ordination Compounds" (Wiley, New York, 1978).
29. H. SUZUKI, H. SAITO, Y. TOMOKIYO and Y. SUAMA, in "Ceramic Transactions" Vol. 6, Mullite and Mullite Matrix Composites, edited by S. Somiya, R. F. Davis and J. A. Pask (The American Ceramic Society, Westerville, Ohio, 1990) p. 263.
30. W. E. CAMERON, *Amer. Ceram Soc. Bull.* **56** (1977) 1003.
31. K. OKADA, Y. HOSHI and N. OTSUKA, *J. Mater. Sci. Lett.* **5** (1986) 1315.
32. G. PRAVDIC and M. S. GANI, *J. Mater. Sci.* **31** (1996) 3487.
33. G. L. MESSING, S.-C. ZHANG and G. V. JAYANTHI, *J. Amer. Ceram. Soc.* **76** (1993) 2707.
34. S.-C. ZHANG, G. L. MESSING and M. BORDEN, *ibid.* **73** (1990) 61.

Received 4 October 2000
and accepted 21 September 2001